

## Directional solidification with buoyancy in systems with small segregation coefficient

G. W. Young

*Department of Mathematics, University of Akron, Akron, Ohio 44304*

S. H. Davis

*Department of Engineering Sciences and Applied Mathematics, Northwestern University, Evanston, Illinois 60201*

(Received 9 January 1986)

We derive an evolution equation governing the cellular structure of a binary alloy having a small segregation coefficient. This equation, applicable to long-wave instabilities of a planar interface, incorporates coupled morphological instabilities and buoyancy effects. The presence of buoyancy can inhibit the onset of the cellular structure by effectively magnifying the segregation and diffusion.

### I. INTRODUCTION

The evolution of pattern in the directional solidification of a solid from its melt is an indicator of the small-scale transitions that determine the physical and electrical properties of the resulting materials. The corrugations of a planar front can amplify, creating complex three-dimensional cellular structures, dendrites with their side branches, and, together with the induced convective flows, the field of microsegregation that determines the distribution of solute in the solid.

Mullins and Sekerka<sup>1,2</sup> analyze the linear stability theory that gives conditions for the corrugations to amplify. Wollkind and Segel<sup>3</sup> fix the wave number and use bifurcation theory to examine weakly nonlinear interactions near the critical point. Such studies have been generalized and extended by Langer and Turski<sup>4</sup> and Langer.<sup>5</sup> Ungar, Brown, and their associates<sup>6-8</sup> have used finite-element numerical simulations of two-dimensional cells to delve into the large-amplitude deformations associated with interactions that are not weakly nonlinear. Figure 1 is drawn from an early photograph of Jackson<sup>9</sup> showing the cellular structure.

In the presence of buoyancy the morphological instability described above can be accompanied by convective effects, given that the solute rejected gives rise to density changes in the melt. On the one hand, unwanted convection can itself lead to undesirable solute redistribution that further degrades the material properties of the solid. On the other hand, it may be possible that convection can reorganize the conditions at the solidification front by removing latent heat and smearing the concentration boundary layer; in this case its presence would be desirable. Coriell *et al.*<sup>10,11</sup> and Hurle *et al.*<sup>12,13</sup> investigate the coupling between the convective and morphological instabilities via linear stability theory. Jenkins<sup>14</sup> and Caroli *et al.*<sup>15</sup> use bifurcation theory to analyze this weakly nonlinear coupling. The conclusion from all these studies is that the coupling is weak due to the fact that the two instabilities individually occur at widely different wave numbers, the disparity in scale precluding a stronger interaction. Nearly all such studies focus on the lead-tin system with segregation coefficient  $k \approx 0.3$ . Here  $k$  is de-

finied by

$$k = C_s / C_f, \quad (1.1)$$

where  $C_s$  is the concentration of solute in the solid and  $C_f$  is that concentration in the liquid at the interface.

If one contemplates the numerical solution of systems involving directional solidification, one must confront the difficulties of three-dimensional free-boundary problems. Further, there is the practical difficulty of dealing with systems having many parameters (normally between 10 and 20) and the subsequent inability to appraise the physics when parameters vary. In order to bypass such difficulties, we shall take an approach suggested by Sivashinsky.<sup>16</sup> He examines the characteristic equation of the linear stability theory of Mullins and Sekerka<sup>2</sup> and sees for small values of  $k$ , that the system has long-wave instabilities. He then develops a long-wave evolution equation for the interface shape whose solution displays cellular structure. This approach has the advantages that the description of the system reduces to a generic partial differential equation containing a single parameter; no free-boundary problem arises. Furthermore, systems with  $k < 0.01$  have great practical interest since they become nearly pure substances upon solidification. The purification of silicon depends upon the rejection of trace contaminants at the solidifying front. The doping of pure sub-

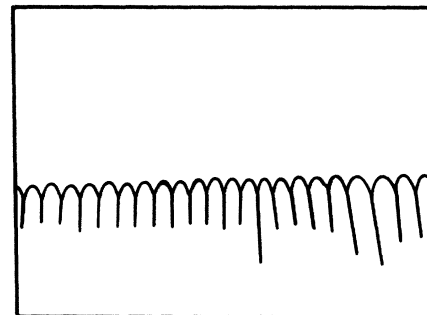


FIG. 1. A drawing of the cellular structure observed by Jackson (Ref. 9), which developed during the directional solidification of a  $\text{CBr}_4$  melt with impurities.

stances with small quantities of solute is used to change the material properties of the final alloy product. Additionally, these systems are commonly used in experiments since it is easy to instigate instabilities in the interface for further investigation by adding small amounts of contaminants.

Here we examine the coupled morphological-convective system for directional solidification for  $k \ll 1$  and for small wave number  $a$ . We formulate the problem in Sec. II, introduce the scalings in Sec. III, and examine linear stability theory in Sec. IV. In Sec. V we give some justification for the approximations made, and in Sec. VI derive the long-wave evolution equation appropriate to weakly nonlinear interactions. In Sec. VII we present some numerical simulations and discuss the results. We find that it is indeed possible, under certain conditions, to suppress morphological instabilities through buoyancy even though sustained convection is absent. The physics of this effect is discussed.

## II. FORMULATION

As shown in Fig. 2, a binary-alloy melt is directionally solidified at constant speed  $V$ . Following Wollkind and Segel<sup>3</sup> and Langer,<sup>17</sup> we assume that the thermal diffusivity  $\kappa$  of the system is much larger than the mass diffusivity  $D$  of the solute, and that the latent heat is not too large. Furthermore, we assume that the thermal conductivities,  $k_L$  and  $k_S$ , in the liquid and solid phases, respectively, are equal. Under these conditions we may neglect the heat generated at the solidifying front and presume that interfacial perturbations do not give rise to disturbances of the temperature field. Thus, the temperature field may be taken as fixed and equal to

$$T = T_0 + Gz. \quad (2.1)$$

Here  $z=0$  is the mean position of the interface,  $T_0$  is the reference temperature of the undisturbed planar interface, and  $G$  is the imposed temperature gradient.

In a frame of reference moving at the velocity  $V$ , the Boussinesq equations for conservation of momentum, mass, and solute in the melt are

$$\mathbf{u}_t + (\mathbf{u} \cdot \nabla) \mathbf{u} - V \mathbf{u}_z = -\frac{\nabla p}{\rho_0} + \nu \nabla^2 \mathbf{u} + \frac{\delta \rho}{\rho_0} \mathbf{g} \mathbf{k}, \quad (2.2)$$

$$\nabla \cdot \mathbf{u} = 0, \quad (2.3)$$

$$c_t + \mathbf{u} \cdot \nabla c - V c_z = D \nabla^2 c, \quad (2.4)$$

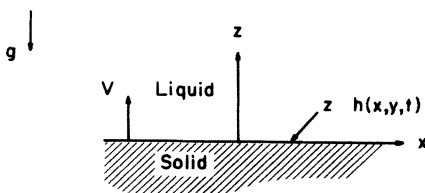


FIG. 2. Schematic of the directional solidification of a melt at speed  $V$ .

where  $\mathbf{u}$  is the fluid velocity,  $p$  the reduced fluid pressure,  $\rho_0$  a reference density,  $c$  the mass concentration of solute in the fluid, and  $\nu$  is the kinematic viscosity of the fluid. We neglect any diffusion of the solute in the solid phase. We also assume that density change  $\delta \rho$  satisfies

$$\frac{\delta \rho}{\rho_0} = \beta(c - C_f), \quad (2.5)$$

where  $\beta$  is the solutal coefficient of expansion,  $\beta > 0$ , and  $C_f$  is the concentration of solute in the fluid at the interface. Here we have neglected the thermal contribution to the density gradient so that solute gradients are the dominant factor determining the convective stability of the system.<sup>13,14</sup>

The mean position of the interface is given by  $z = h(x, y, t)$ . There are the no slip conditions and the mass balance condition

$$\mathbf{u} = \mathbf{0}, \quad (2.6)$$

assuming that the density change upon solidification is negligible. There is conservation of solute at the interface

$$c(1-k)(V + h_t) = -D(c_z - c_x h_x - c_y h_y), \quad (2.7)$$

and there is the condition of thermodynamic equilibrium

$$T = mc + T_M \left[ 1 + \frac{\gamma}{L} K \right]. \quad (2.8)$$

Since  $T$  is given by (2.1), we have

$$T_0 + Gh = mc + T_M \left[ 1 + \frac{\gamma}{L} K \right]. \quad (2.9)$$

Here, from the phase diagram of Fig. 3,  $m$  is the liquidus slope,  $T_M$  is the melting point of the pure substance,  $\gamma$  is the surface free energy,  $L$  is the latent heat, and  $K$  is twice the mean curvature

$$K = [h_{xx}(1+h_y^2) - 2h_x h_y h_{xy} + h_{yy}(1+h_x^2)] \times (1+h_x^2+h_y^2)^{-3/2}. \quad (2.10)$$

Faraway from the interface, we assume that the velocity field is bounded and that the solute concentration is  $C_s$ , the concentration of the solute in the solid phase.

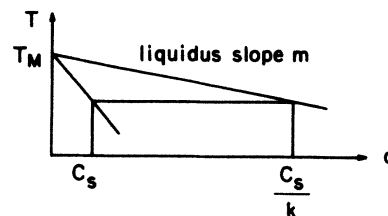


FIG. 3. The phase diagram:  $C_s/k$  represents the concentration of solute in the liquid at the interface while  $C_s$  represents the concentration in the solid, both occurring at the same temperature.

III. BASIC STATE AND SCALING

There exists a steady-state solution, with a planar interface,  $h \equiv 0$ , and zero melt velocity,  $\mathbf{u} \equiv \mathbf{0}$ , to the above system. This temperature field is

$$T = T_0 + Gz, \tag{3.1}$$

where from Eq. (2.9) the reference temperature of the planar interface is

$$T_0 = \frac{mC_s}{k} + T_M. \tag{3.2}$$

The concentration field is

$$c = \frac{C_s}{k} + \frac{G_c D}{V} \left[ 1 - \exp \left[ -\frac{Vz}{D} \right] \right], \tag{3.3}$$

where  $G_c$  is the solute gradient at the interface,

$$G_c = \frac{(k-1)C_s V}{kD}, \tag{3.4}$$

based upon the concentration boundary-layer thickness  $\delta$ ,

$$\delta = D/V. \tag{3.5}$$

We now scale all lengths in the system with  $\delta$ , velocities with  $V$ , time with the characteristic time for diffusion,  $D/V^2$ , concentration with  $\delta G_c$ , and the pressure with  $\mu V^2/D$ , consistent with a slow viscous flow in the melt. The scaled variables, denoted by primes, are

$$\begin{aligned} x &= \delta x', \quad y = \delta y', \quad z = \delta z', \quad h = \delta h', \\ u &= Vu', \quad v = Vv', \quad w = Vw', \quad p = \frac{\mu V^2}{D} p', \\ t &= \frac{D}{V^2} t', \quad c - \frac{C_s}{k} = \frac{G_c D}{V} c'. \end{aligned} \tag{3.6}$$

These scalings give rise to the following nondimensional groups. There is the Schmidt number

$$S = \frac{\nu}{D} \tag{3.7}$$

the morphological parameter  $M$ ,

$$M = \frac{mG_c}{G}, \tag{3.8}$$

which measures the degree of constitutional supercooling at the interface,

$$\Gamma = \frac{T_M \gamma}{LmG_c} \left[ \frac{V}{D} \right]^2, \tag{3.9}$$

which measures the effects of the surface free energy, and the solute Rayleigh number

$$R = \frac{-g\beta G_c}{\nu D} \left[ \frac{D}{V} \right]^4 = \frac{(1-k)C_s g\beta}{k\nu D} \left[ \frac{D}{V} \right]^3. \tag{3.10}$$

$R$  measures the strength of the buoyant force due to solute being rejected at the interface. For definiteness it is assumed that the solute is less dense than the solvent and thus, as shown in Fig. 4, we have a potentially unstable

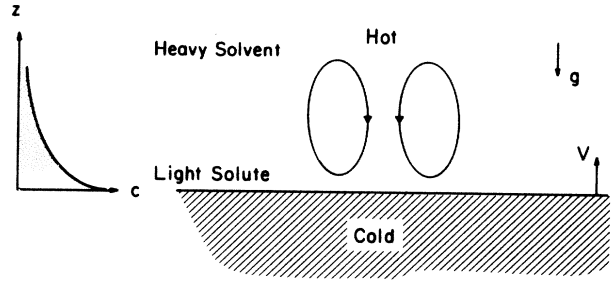


FIG. 4. The rejection of light solute at the solidifying interface beneath the heavy solvent away from the interface may lead to a convective instability.

situation with light solute beneath heavy solvent. The minus sign in the definition of  $R$  is due to the fact that  $G_c < 0$  for  $k < 1$ .

If we substitute (3.6) into system (2.2)–(2.4), (2.6)–(2.9), and drop the primes, the governing equations become

$$S^{-1}[\mathbf{u}_t + (\mathbf{u} \cdot \nabla)\mathbf{u} - \mathbf{u}_z] = -\nabla p + \nabla^2 \mathbf{u} - Rc \hat{\mathbf{k}}, \tag{3.11}$$

$$\nabla \cdot \mathbf{u} = 0, \tag{3.12}$$

$$c_t + \mathbf{u} \cdot \nabla c - c_z = \nabla^2 c, \tag{3.13}$$

subject to the boundary conditions at the interface  $z = h(x, y, t)$ ,

$$\mathbf{u} = \mathbf{0}, \tag{3.14}$$

$$[c(k-1) + 1](1 + h_t) = c_z - h_x c_x - h_y c_y, \tag{3.15}$$

$$c - M^{-1}h + \Gamma [h_{xx}(1 + h_y^2) - 2h_x h_y h_{xy} + h_{yy}(1 + h_x^2)] \times (1 + h_x^2 + h_y^2)^{-3/2} = 0, \tag{3.16}$$

and conditions far from the interface as  $z \rightarrow \infty$ ,

$$|\mathbf{u}| < \infty, \tag{3.17}$$

$$c = 1. \tag{3.18}$$

The scaled basic state is

$$\bar{u}, \bar{v}, \bar{w} \equiv 0, \tag{3.19a}$$

$$\bar{h} \equiv 0, \tag{3.19b}$$

$$\bar{c} = 1 - e^{-z}. \tag{3.19c}$$

We can eliminate the dependence upon the pressure field in Eq. (3.11) by taking the curl of that equation twice to obtain

$$S^{-1} \left[ \frac{\partial}{\partial t} \nabla^2 \mathbf{u} - \nabla(\nabla \cdot (\mathbf{u} \cdot \nabla)\mathbf{u}) + \nabla^2(\mathbf{u} \cdot \nabla)\mathbf{u} - \frac{\partial}{\partial z} \nabla^2 \mathbf{u} \right] = \nabla^4 \mathbf{u} - R D c. \tag{3.20}$$

Here

$$\mathbf{D} = \left[ -\frac{\partial^2}{\partial x \partial z}, -\frac{\partial^2}{\partial y \partial z}, \frac{\partial^2}{\partial x^2} + \frac{\partial^2}{\partial y^2} \right]. \tag{3.21}$$

We also note that using (3.12) and (3.14) we have

$$w_z = 0 \quad (3.22)$$

at the interface. The Eqs. (3.20) and (3.22) will be convenient to use for the linear stability analysis to follow.

#### IV. LINEAR STABILITY ANALYSIS

We now allow disturbances to the basic state as follows:

$$(u, v, w) = (0, 0, 0) + \epsilon(U, V, W), \quad (4.1a)$$

$$h = 0 + \epsilon H, \quad (4.1b)$$

$$c = 1 - e^{-z} + \epsilon C. \quad (4.1c)$$

We substitute (4.1) into the scaled system (3.3)–(3.18), (3.20), and (3.22) and linearize with respect to  $\epsilon$ . For each dependent variable  $\psi$  we introduce normal modes as follows:

$$\psi(x, y, z, t) = \Psi(z)\Phi(x, y)e^{\sigma t}, \quad (4.2)$$

where the growth rate  $\sigma$  determines the stability of the basic state, and  $\Phi$  satisfies

$$\Phi_{xx} + \Phi_{yy} + a^2\Phi = 0 \quad (4.3)$$

and  $a$  is the disturbance wave number.

The growth rate  $\sigma$  is an eigenvalue of the system

$$\left[ \frac{d^2}{dz^2} - a^2 \right] \left[ \frac{d^2}{dz^2} + S^{-1} \frac{d}{dz} - a^2 - S^{-1}\sigma \right] W = -a^2 RC, \quad (4.4)$$

$$\left[ \frac{d^2}{dz^2} + \frac{d}{dz} - a^2 - \sigma \right] C = W e^{-z}, \quad (4.5)$$

subject to the following boundary conditions applied at the undisturbed interfacial position  $z=0$ ,

$$W = W_z = 0, \quad (4.6a)$$

$$\frac{dC}{dz} + (1-k)C - (\sigma+k)H = 0, \quad (4.6b)$$

$$-C + (M^{-1}-1)H + a^2\Gamma H = 0, \quad (4.6c)$$

and faraway from the interface as  $z \rightarrow \infty$ ,

$$|W| < \infty, \quad (4.7a)$$

$$C \rightarrow 0. \quad (4.7b)$$

One can solve the linearized thermodynamic equilibrium equation (4.6c) for the interfacial perturbation  $H$  to find that

$$H = \frac{C}{M^{-1}-1+a^2\Gamma}. \quad (4.8)$$

Furthermore, if  $M \rightarrow 0$ , then (4.8) requires that  $H \rightarrow 0$ , which is the unperturbed state. This is consistent with (3.8) since if the undercooling is zero, then there will be no morphological instability.

Now if we substitute for  $H$  in (4.6b), using (4.8), the mass conservation of solute at the interface equation becomes

$$\frac{dC}{dz} + (1-k)C - \frac{(\sigma+k)C}{M^{-1}-1+a^2\Gamma} = 0, \quad (4.9)$$

the last term of which represents a perturbation in the concentration field due to an interfacial-shape change. If  $M \rightarrow 1$ , which is near the critical value for instability, then this term is proportional to  $a^{-2}$ . If  $a$  were small, then this term would dominate the diffusional term  $dC/dz$ ; this is a singular perturbation. Since  $a$  is the disturbance wave number, then the dimensional wavelength or characteristic cell size of an interfacial perturbation is

$$\lambda = \frac{D}{V} \frac{2\pi}{a}. \quad (4.10)$$

Small  $a$  would imply that the cell size exceeds the diffusional width  $D/V$  of the solidification zone. Such may be the case particularly at the onset of instability near  $M=1$ .

Thus, we assume that

$$a \ll 1 \quad (4.11)$$

and rescale the problem for systems with small  $k$  as follows:

$$k = a^2 \tilde{k}, \quad (4.12a)$$

$$\sigma = a^2 \tilde{\sigma}. \quad (4.12b)$$

This scaling retains the last term of (4.9) as an order one quantity near  $M=1$ .

The governing system becomes

$$\left[ \frac{d^2}{dz^2} - a^2 \right] \left[ \frac{d^2}{dz^2} + S^{-1} \frac{d}{dz} - a^2(1+S^{-1}\tilde{\sigma}) \right] W = -a^2 RC, \quad (4.13)$$

$$\left[ \frac{d^2}{dz^2} + \frac{d}{dz} - a^2(1+\tilde{\sigma}) \right] C = W e^{-z} \quad (4.14)$$

subject to conditions at  $z=0$ ,

$$W = W_z = 0, \quad (4.15a)$$

$$\frac{dC}{dZ} + (1-a^2\tilde{k})C - \frac{a^2(\tilde{\sigma}+\tilde{k})C}{M^{-1}-1+a^2\Gamma} = 0, \quad (4.15b)$$

and conditions (4.7a) and (4.7b) far from the interface.

We assume a power-series expansion for all dependent variables in the problem,

$$W = W_0 + a^2 W_1 + \dots, \quad (4.16a)$$

$$C = C_0 + a^2 C_1 + \dots \quad (4.16b)$$

and substitute these into (4.15)–(4.17).

The solution procedure is straightforward and we find at leading order that

$$W_0 = 0, \quad (4.17a)$$

$$C_0 = A e^{-z}, \quad (4.17b)$$

where  $A$  is an arbitrary constant of integration.

At order  $a^2$  we obtain

$$W_1 = RSA \left[ -1 + \frac{1}{S-1} (Se^{z/S} - e^{-z}) \right], \quad (4.18a)$$

$$C_1 = Be^{-z} A \left[ (RS - \tilde{\sigma} - 1)ze^{-z} - \frac{RS}{2(S-1)} e^{-2z} + \frac{RS^4}{S^2-1} \exp \left[ -\frac{(1+S)z}{S} \right] \right], \quad (4.18b)$$

where  $B$  is an arbitrary constant of integration.

We now substitute  $C_1$  into the  $O(a^2)$  part of (4.15b),

$$\frac{dC_1}{dz} + C_1 = A\tilde{k} + \frac{(\tilde{\sigma} + \tilde{k})A}{M^{-1} - 1 + a^2\Gamma}, \quad (4.19)$$

and obtain an expression for the linear-theory growth rate  $\sigma$ . If we now use (4.12a) and (4.12b), we find

$$\sigma = \left[ \frac{(1 - M^{-1})a^2 - a^4\Gamma}{M^{-1} + a^2\Gamma} \right] \left[ 1 - \frac{R}{2(1 + S^{-1})} \right] - k. \quad (4.20)$$

When gravity is absent,  $R = 0$ . If we examine  $M$  near unity, and  $a^2$  small, the expression (4.20) reduces to

$$\sigma = (1 - M^{-1})a^2 - a^4\Gamma - k \quad (4.21)$$

which, except for notation, is identical to that of Sivashinsky,<sup>16</sup> who considers the morphological instability of systems with small  $k$ , near  $M = 1$ , in the absence of buoyancy. We recover this limit since  $W_1 = 0$  for  $R = 0$  as shown in (4.18a). Thus (4.20) extends Sivashinsky's results to include the effects of buoyancy.

We can calculate from (4.20) the critical  $R$  and  $a$  when  $\sigma = 0$  to obtain

$$R_c = 2(1 + S^{-1})[1 - k\Gamma(1 - M^{-1/2})^{-2}] \quad (4.22a)$$

and

$$a_c^2 = M^{-1}\Gamma^{-1}(M^{1/2} - 1). \quad (4.22b)$$

If we take the limit  $M \rightarrow 0$  in (4.22a) we find that

$$R_c = 2(1 + S^{-1}), \quad (4.23)$$

which agrees with Hurle *et al.*,<sup>13</sup> who consider the convective stability of the melt motion for a system with  $k \rightarrow 0$  and a planar interface (in the absence of morphological instability). Since  $M^{-1}$  and  $\Gamma$  are inversely proportional to the concentration  $C_s$  of solute, then increasing  $C_s$  increases the wave number of the instability. A pure substance,  $C_s = 0$ , has wave number equaling zero, which gives a planar interface.

In Fig. 5 we plot from Eq. (4.20) the growth rate versus wave number for various values of  $R$ . Recall that  $\sigma > 0$  implies instability while  $\sigma < 0$  gives stability. From (4.21) if  $M > 1$ , then the contribution to  $\sigma$  due to undercooling is positive and thus the system is susceptible to a morphological instability. On the other hand, the presence of surface free energy  $\Gamma$  and an increasing  $k$  imply a smaller concentration gradient, and therefore are stabilizing effects. Thus if  $k$  is not too large, then for  $R = 0$ ,  $\sigma > 0$  for a range of wave numbers  $a$  and the system is morphologi-

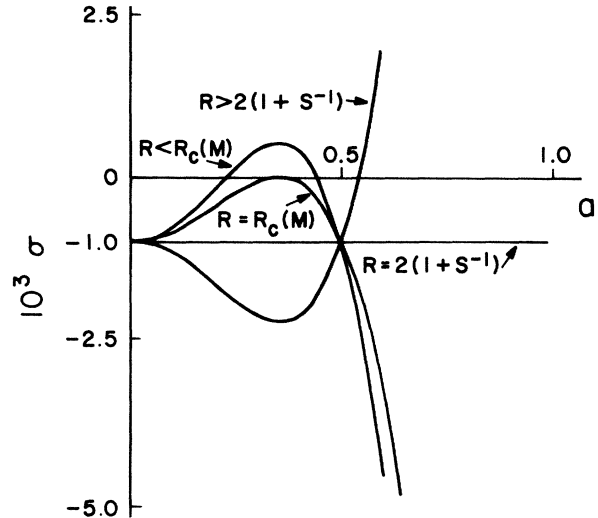


FIG. 5. Plot of the growth rate expression (4.20). Here  $M = 1.025$ ,  $k = 0.001$ ,  $S = 10.0$ ,  $\Gamma = 0.1$ , and  $R_c$  is given by (4.22a).

cally unstable as shown in Fig. 5.

Now as the buoyant force is increased by raising  $R$ , the morphological instability is damped. When

$$R_c < R < 2(1 + S^{-1}), \quad (4.24)$$

the system is stabilized even though  $M > 1$ . Caroli *et al.*<sup>15</sup> also find that the coupling of buoyancy stabilizes the solidifying front. Their result is valid for a Pb-Sn system where the wave number is not small. They do note, however, for small wave numbers, that the effective Rayleigh number for the problem is  $a^2R$  which agrees with (4.13). However, they do not pursue this limit since it is not physically relevant for the Pb-Sn system.

When  $R > 2(1 + S^{-1})$  in (4.20), the buoyant force is strong enough to cause a sustained convective instability in the system. This instability has wave number greater than  $a_c$  of Eq. (4.22b), which as shown in Fig. 5 may be unit order and thus outside the range of the present theory. Furthermore, the quantity  $a^2R$  may be greater than  $O(a^2)$  in this region, which is also inconsistent with the theory.

The above results are summarized in Fig. 6. The tongue of stability near  $R = 2(1 + S^{-1})$  shown for large  $M$  is as wide as the correction to  $R_c = 2(1 + S^{-1})$  given in (4.22a). Since it is proportional to  $k$ , and  $k$  is small, then it is unlikely that such a region could be found experimentally. However, near  $M = 1$ , the region of stability is larger. Furthermore, this region occurs for  $R < 2(1 + S^{-1})$  so that the system attains at long times a static configuration; no sustained convection is possible.

In order to determine the mechanism by which buoyancy is able to suppress the morphological instability, a non-linear analysis is required to completely specify the velocity and concentration fields. The linear analysis discussed above does not determine the arbitrary constants of integration,  $A$  and  $B$  of (4.17) and (4.18).

Before turning to this task, we pause a moment to examine in detail the approximations made and their physical implications.

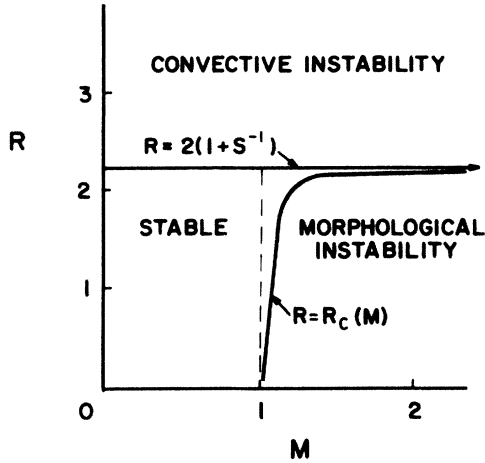


FIG. 6. Plot in the  $R$  vs  $M$  plane of the results shown in Fig. 5.

### V. APPROXIMATIONS

For purposes of this discussion let us take  $R=0$ . When  $M$  is near unity,  $M-1=O(a^2)$ , the linear theory growth rate  $\sigma$  is obtained from Eq. (4.21),

$$\sigma \sim (M-1)a^2 - a^4\Gamma - k, \quad (5.1)$$

while the critical wave number  $a_c$  is obtained from Eq. (4.22b),

$$a_c^2 \sim \frac{1}{2\Gamma}(M-1). \quad (5.2)$$

Thus maximizing the wave number corresponds to an unstable disturbance if

$$k < \frac{1}{4\Gamma}(M-1)^2 \ll 1. \quad (5.3)$$

Now, the asymptotic expansions (4.16) require that

$$a^2 \ll 1, \quad (5.4)$$

so from form (5.2) we must have

$$\frac{1}{2\Gamma}(M-1) \ll 1. \quad (5.5)$$

The scalings in the nonlinear problem described in Sec. VI require that

$$k/\Gamma = O(a^4) \quad (5.6)$$

which is consistent with (5.3) and agrees with the small- $k$  limit of the wave number found by Sekerka.<sup>18</sup>

Further, we have assumed that the effects of latent heat are negligible and that the thermal conductivities  $k_S$  and  $k_L$  in the solid and liquid, respectively, are equal. The former of these requires that

$$\frac{VL}{k_L G} \ll 1, \quad (5.7)$$

while condition (5.3) requires that  $\Gamma$  not be too small.

The present analysis should apply to materials having

small segregation coefficient  $k$ , small latent heat  $L$ , large surface free energy  $\gamma$ , and small solute diffusion coefficient  $D$ . For a given binary system, choose  $V$  and  $G$  to satisfy (5.7). The magnitude of  $\Gamma$  defines the closeness of  $M$  to unity, through inequality (5.3), and hence the size of  $k$ . Note that  $k \ll (1/4\Gamma)(M-1)^2$  is *not* required. Note also that inequality (5.4) requires  $a^2$  small, not  $a$ . Consider now a system for which  $\Gamma = 10^{-1}$  and  $k = 10^{-3}$ . Then we have a long-wave instability with  $a^2 \approx 10^{-1}$  as long as  $0 \leq M-1 < 2 \times 10^{-2}$ . Alternatively, if  $\Gamma = 10^{-3}$  and  $k = 10^{-5}$ , there is an instability with  $a^2 = 10^{-1}$  as long as  $0 \leq M-1 < 2 \times 10^{-4}$ . Such situations seem reasonable when silicon or germanium with trace contaminants are processed.

### VI. WEAKLY NONLINEAR ANALYSIS

In order to obtain the weakly nonlinear behavior of the system, define

$$M = 1 + \epsilon, \quad \epsilon \ll 1, \quad (6.1)$$

where parameter  $\epsilon$  measures the degree of the undercooling. Following Sivashinsky,<sup>16</sup> we rescale the original governing equations (3.11)–(3.19) as follows:

$$x\epsilon^{1/2} = X, \quad y\epsilon^{1/2} = Y, \quad z = Z, \quad h = \epsilon H, \quad c = C, \quad (6.2)$$

$$\epsilon^2 \bar{k} = k, \quad t\epsilon^2 = T, \quad \epsilon^{1/2}u = U, \quad \epsilon^{1/2}v = V, \quad w = W.$$

These scalings are determined by using (6.1) and the linear theory of Sec. IV.

For ease of discussion *only* we examine the two-dimensional case,  $V=0$ ,  $\partial/\partial Y=0$ . In terms of the stream function  $\psi$  such that

$$U = -\psi_Z, \quad W = \psi_X, \quad (6.3)$$

the governing equations are

$$S^{-1} \left[ \left[ \epsilon^2 \frac{\partial}{\partial T} + \psi_X \frac{\partial}{\partial Z} - \psi_Z \frac{\partial}{\partial X} \right] (\epsilon \psi_{XX} + \psi_{ZZ}) \right] \\ = \left[ \epsilon \frac{\partial^2}{\partial X^2} + \frac{\partial^2}{\partial Z^2} \right] (\epsilon \psi_{XX} + \psi_{ZZ}) - \epsilon RC_X, \quad (6.4)$$

$$\epsilon^2 C_T - \psi_Z C_X + \psi_X C_Z - C_Z = \epsilon C_{XX} + C_{ZZ} \quad (6.5)$$

subject to boundary conditions at the interface  $Z = \epsilon H(X, T)$ ,

$$\psi = \psi_Z = 0, \quad (6.6a)$$

$$[C(\epsilon^2 \bar{k} - 1) + 1](1 + \epsilon^3 H_T) = C_Z - \epsilon^2 H_X C_X, \quad (6.6b)$$

$$C - \epsilon H(1 + \epsilon)^{-1} + \epsilon^2 \Gamma H_{XX}(1 + \epsilon^2 H_X^2)^{-3/2} = 0, \quad (6.6c)$$

and boundary conditions as  $Z \rightarrow \infty$

$$|\psi| < \infty, \quad (6.7a)$$

$$C \rightarrow 1. \quad (6.7b)$$

We seek solutions in powers of  $\epsilon$  as follows:

$$\psi = 0 + \epsilon\psi_1 + \epsilon^2\psi_2 + \dots, \quad (6.8a)$$

$$C = 1 - \epsilon^{-Z} + \epsilon C_1 + \epsilon^2 C_2 + \dots, \quad (6.8b)$$

$$H = H_0 + \epsilon H_1 + \dots. \quad (6.8c)$$

The leading-order problem is identically satisfied by the basic state. At  $O(\epsilon)$  we find that  $\psi_1 = C_1 \equiv 0$ .

At  $O(\epsilon^2)$  we have

$$-S^{-1}\psi_{2,ZZZ} = \psi_{2,ZZZZ}, \quad (6.9a)$$

$$\psi_{2,X}e^{-Z} - C_{2,Z} = C_{2,ZZ}, \quad (6.9b)$$

$$\psi_2 = \psi_{2,Z} = 0, \quad Z = 0 \quad (6.10a)$$

$$C_{2,Z} + C_2 = 0, \quad Z = 0 \quad (6.10b)$$

$$C_2 - \frac{1}{2}H_0^2 + H_0 + \Gamma H_{0,XX} = 0, \quad Z = 0 \quad (6.10c)$$

$$\psi_2 \text{ bounded}, \quad Z \rightarrow \infty \quad (6.11a)$$

$$C_2 \rightarrow 0, \quad Z \rightarrow \infty. \quad (6.11b)$$

Equation (6.9a), subject to boundary conditions (6.10a) and (6.11a), implies that

$$\psi_2 = 0. \quad (6.12)$$

We then solve for the concentration field  $C_2$  using (6.9b), (6.10b), (6.10c), and (6.11b) to find that

$$C_2 = \alpha e^{-Z}, \quad (6.13)$$

where

$$\alpha = \frac{1}{2}H_0^2 - H_0 - \Gamma H_{0,XX}. \quad (6.14)$$

However, to this order, the interfacial position  $H_0$  is still unknown, so that we must examine the  $O(\epsilon^3)$  problem:

$$\psi_{3,ZZZZ} + S^{-1}\psi_{3,ZZZ} = R\alpha_X e^{-Z}, \quad (6.15a)$$

$$C_{3,ZZ} + C_{3,Z} = \psi_{3,X}e^{-Z} - \alpha_{XX}e^{-Z}, \quad (6.15b)$$

$$\psi_3 = \psi_{3,Z} = 0, \quad Z = 0 \quad (6.16a)$$

$$C_{3,Z} + C_3 = H_{0,T} + \bar{k}H_0, \quad Z = 0 \quad (6.16b)$$

$$\psi_3 \text{ bounded}, \quad Z \rightarrow \infty \quad (6.17a)$$

$$C_3 \rightarrow 0, \quad Z \rightarrow \infty. \quad (6.17b)$$

Equations (6.15a), (6.16a), and (6.17a) give

$$\psi_3 = SR\alpha_X \left[ 1 - \frac{S}{S-1}e^{-Z/S} + \frac{e^{-Z}}{S-1} \right], \quad (6.18)$$

while (6.15b) and (6.17b) give

$$C_3 = \Delta e^{-Z} + \alpha_{XX} \left[ (1-SR)Ze^{-Z} + \frac{SR}{2(S-1)}e^{-2Z} - \frac{RS^4}{S^2-1} \exp \left[ -\frac{(1+S)}{S}Z \right] \right], \quad (6.19)$$

where  $\Delta$  is an unknown function of integration.  $\Delta$  is determined through the  $O(\epsilon^3)$  contribution of (6.6c). By substituting (6.19) into (6.16b), we obtain an evolution equation for the interfacial shape  $H_0$ , independent of  $\Delta$ ,

$$H_{0,T} + \bar{k}H_0 + \{ \Gamma H_{0,XXXX} + [(1-H_0)H_{0,X}]_X \}$$

$$\times \left[ 1 - \frac{R}{2(1+S^{-1})} \right] = 0. \quad (6.20)$$

Equation (6.20) agrees with the result of Sivashinsky<sup>16</sup> in the case  $R=0$  and upon rescaling gives a *single parameter*  $k\Gamma\epsilon^{-2}$  governing the behavior.

Whenever  $R < 2(1+S^{-1})$ , sustained convection is absent and the transformation

$$H_0 = F, \quad T = \frac{\Gamma\tau}{\left| 1 - \frac{R}{2(1+S^{-1})} \right|}, \quad X = \Gamma^{1/2}\xi \quad (6.21)$$

converts Eq. (6.20) into the following one-parameter form of the evolution equation:

$$F_\tau + KR + F_{\xi\xi\xi\xi} + [(1-F)F_\xi]_\xi = 0, \quad (6.22)$$

where

$$K = \frac{k\Gamma}{\epsilon^2 \left| 1 - \frac{R}{2(1+S^{-1})} \right|}. \quad (6.23)$$

In three dimensions, one obtains the obvious generalization

$$F_\tau + KR + \nabla^4 F + \nabla \cdot [(1-F)\nabla F] = 0, \quad (6.24)$$

where

$$\nabla = \frac{\partial}{\partial \xi} \hat{\mathbf{i}} + \frac{\partial}{\partial \eta} \hat{\mathbf{j}} \quad (6.25a)$$

and

$$Y = \Gamma^{1/2}\eta. \quad (6.25b)$$

Clearly, the presence of buoyancy (without sustained convection) leads to an effective segregation coefficient  $K$ , given by Eq. (6.23), larger than the physicochemical value  $k$  by an amount determined by the Rayleigh number. This will be discussed further in Sec. VII.

When  $R > 2(1+S^{-1})$ , the evolution equation is quantitatively different, having the form

$$F_\tau + KR - \nabla^4 F - \nabla \cdot [(1-F)\nabla F] = 0. \quad (6.26)$$

Here, now what were stabilizing fourth-order and destabilizing second-order terms, have their roles interchanged.

## VII. RESULTS

Let us return to the two-dimensional problem (6.22) subject to periodic boundary conditions on the interval  $\xi=0$  to  $\xi=l$ . Given the solution for  $F$ , one can determine the concentration distribution from

$$C = 1 - e^{-Z} + \epsilon^2 \left( \frac{1}{2}F^2 - F - F_{\xi\xi} \right) e^{-Z} \quad (7.1)$$

obtained from Eqs. (6.8b), (6.13), and (6.21). Since  $Z = \epsilon H(X, T)$ , we can use Eqs. (3.6), (6.8c), and (6.21) to obtain

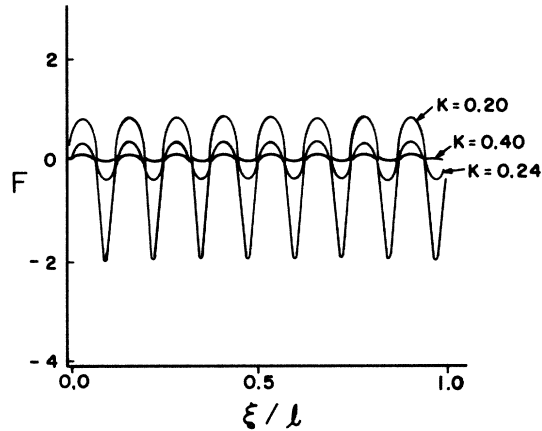


FIG. 7. Numerical simulation of Eq. (6.22) results in the above interfacial shapes for the given values of  $K$ . Here  $l = 16\pi\sqrt{2}$ .

$$c = \frac{C_s}{k} [1 - \epsilon F + \epsilon^2(\bar{k} + F + F_{\xi\xi})]. \quad (7.2)$$

We solve Eq. (6.22) using an explicit finite difference scheme for various values of  $l$  chosen as multiples of the wavelength  $2\pi/a_c = 2\pi\sqrt{2}$  giving maximum amplification in the linear theory of Eq. (6.22). This linear theory gives  $K < \frac{1}{4}$  for instability.

Figure 7 shows the calculated interfacial shape  $F$  for various values of  $K$ . Figure 8 shows the corresponding concentration profiles. The initial condition  $F = 0.25 \sin[2\pi(\xi/l)]$  has been used in all cases. The time integration is performed until the cell tips have reached steady state and the cell slopes are large. The units of the  $F$  axis are proportional to  $\epsilon\delta$  and the units of the  $\xi$  axis are proportional to  $(\Gamma/\epsilon)^{1/2}\delta$ . When  $K > \frac{1}{4}$ , initial disturbances decay to zero and the basic state planar front is regained. When  $K$  is below  $\frac{1}{4}$ , the system is unstable and a cellular structure forms, qualitatively similar in appearance to those of the experiment<sup>9</sup> shown in Fig. 1 and

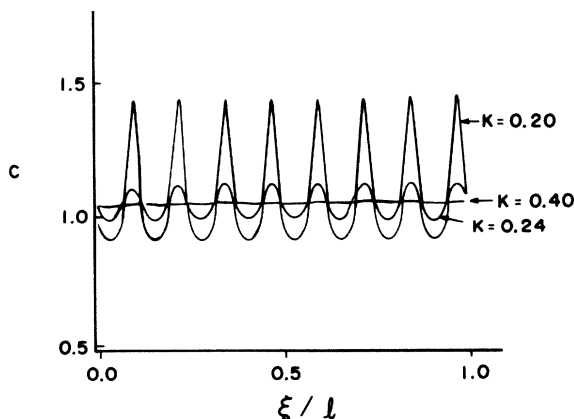


FIG. 8. Plot of the concentration expression (7.2). Here  $\epsilon = 0.2$ ,  $\bar{k} = 1.0$ , and  $C_s/k = 1.0$ .

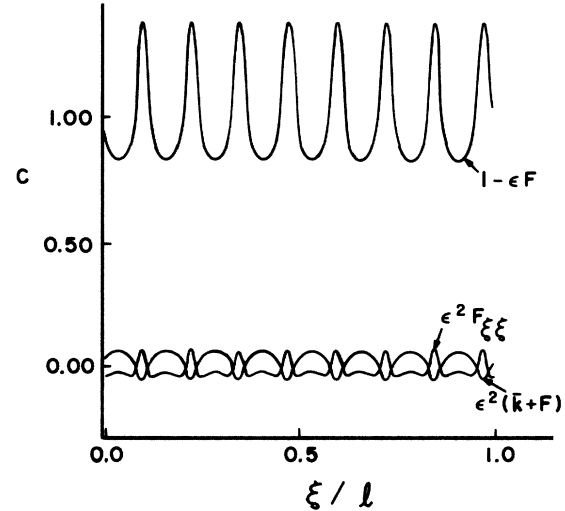


FIG. 9. The component parts of Eq. (7.2).

direct numerical computation.<sup>6-8</sup> (Note that the present long-wave theory should be valid when the cell slopes are bounded and should break down when vertical sections appear. Further, the “droplet-shaped” root tip seen in experiment<sup>9</sup> and detailed numerical simulation<sup>6</sup> should be missing in that fine structure should not be resolvable in this approximation.) The concentration profiles from the linearized version of Eq. (7.2) show that  $c \sim 1 - \epsilon F$ , so that  $c$  is largest where  $F$  is smallest; solute aggregates at the roots. The nonlinear theory shows a further redistribution with the  $F_{\xi\xi}$  term predominant; this term measures the relatively large curvature at the root and distorts the sinusoidal profile of  $c$  consistent with linear theory into the root-flattened concentration profiles shown in Fig. 8. Figure 9 shows the contributions to  $c$  of Eq. (7.2) separated into component parts.

Finally, when Eq. (6.22) is integrated for values of  $K$  significantly smaller than  $\frac{1}{4}$ , the tips of the cells show a tendency to split, an effect perhaps related to the appearance of half-wave secondary bifurcations obtained by Ungar and Brown<sup>6</sup> from a numerical analysis of the full system.

## VIII. DISCUSSION AND CONCLUSIONS

Asymptotic analysis of directional solidification in the presence of buoyancy is possible for small segregation coefficient and long-wave disturbances. The result is a single partial differential equation, the evolution equation that governs the approximate weakly nonlinear behavior of either two or three-dimensional cells as a function of a single nondimensional group  $K$ . When buoyancy is absent so that the Rayleigh number  $R = 0$ ,  $K$  is a scaled version of the segregation coefficient  $k$ . When  $0 < R < 2(1 + S^{-1})$ , sustained convection is absent but buoyancy increases  $K$ , the effective segregation coefficient. According to definition (1.1) and assuming that the concentration  $C_s$  of solute in the solid is constant, then an increase in  $k$  corresponds to a decrease in the concentration of solute in

the liquid at the interface. Thus, the buoyant force acting on the light solute has *enhanced* the diffusion of solute away from the interface. This decreases the concentration gradient, thus lowering the tendency for the liquid to become supercooled. The result is a suppression of the morphological instability.

Numerical integration of the evolution equation in two dimensions shows the quantitative behavior of the system. For  $K < \frac{1}{4}$  cells form and when the amplitudes are infinitesimal, lateral diffusion causes a small solute aggregation at the troughs of the interface. The nonlinearities in Eq. (6.22) accentuate this trend since lateral diffusion is enhanced. The strong distortion of the concentration pro-

file showing solute segregation indicates that the solute is trapped between adjacent cells, the diffusion upwards along the root canal being too slow to accommodate the narrowing of the root canal by solidification. This undesirable distribution would then be frozen into the final crystal product.

#### ACKNOWLEDGMENTS

The authors are grateful for the valuable suggestions made by Mr. K. E. Brattkus. This work was supported by the National Science Foundation, Fluid Mechanics Program.

- 
- <sup>1</sup>W. W. Mullins and R. F. Sekerka, *J. Appl. Phys.* **34**, 323 (1963).  
<sup>2</sup>W. W. Mullins and R. F. Sekerka, *J. Appl. Phys.* **35**, 444 (1964).  
<sup>3</sup>D. J. Wollkind and L. A. Segel, *Philos. Trans. R. Soc. London, Ser. A* **268**, 351 (1970).  
<sup>4</sup>J. S. Langer and L. A. Turski, *Acta Metall.* **25**, 1113 (1977).  
<sup>5</sup>J. S. Langer, *Acta Metall.* **25**, 1121 (1977).  
<sup>6</sup>L. H. Ungar and R. A. Brown, *Phys. Rev. B* **29**, 1367 (1984).  
<sup>7</sup>L. H. Ungar and R. A. Brown, *Phys. Rev. B* **30**, 3993 (1984).  
<sup>8</sup>L. H. Ungar, M. J. Bennett, and R. A. Brown, *Phys. Rev. B* **31**, 5923 (1985).  
<sup>9</sup>K. A. Jackson, in *Solidification*, edited by T. J. Hughel and G. F. Bolling (American Society for Metals, Metal Park, Ohio, 1971), p. 133.  
<sup>10</sup>S. R. Coriell, M. R. Cordes, W. S. Boettinger, and R. F. Sekerka, *J. Cryst. Growth* **49**, 13 (1980).  
<sup>11</sup>S. R. Coriell, G. B. McFadden, R. F. Boisvert, and R. F. Sekerka, *J. Cryst. Growth* **69**, 514 (1984).  
<sup>12</sup>D. T. J. Hurle, E. Jakeman, and A. A. Wheeler, *J. Cryst. Growth* **58**, 163 (1982).  
<sup>13</sup>D. T. J. Hurle, E. Jakeman, and A. A. Wheeler, *Phys. Fluids* **26**, 624 (1983).  
<sup>14</sup>D. R. Jenkins, Ph.D. thesis, University of Cambridge, Cambridge, England, 1984.  
<sup>15</sup>B. Caroli, C. Caroli, C. Misbah, and B. Roulet, *J. Phys. (Paris)* **46**, 401 (1985).  
<sup>16</sup>G. I. Sivashinsky, *Physica* **8D**, 243 (1983).  
<sup>17</sup>J. S. Langer, *Rev. Mod. Phys.* **52**, 1 (1980).  
<sup>18</sup>R. F. Sekerka, *J. Appl. Phys.* **36**, 264 (1965).